1

A THEORY FOR TURBULENT PIPE AND CHANNEL FLOWS

William K. George and Luciano Castillo
State University of New York at Buffalo
Buffalo, NY 14260

November 8, 1996

Abstract

A theory for turbulent pipe and channel flows is proposed based on a similarity analysis of the boundary layer equations. It is argued from dimensional and physical considerations that the proper scaling for these flows near the wall is

$$\frac{U}{u_*} = f\left(y^+, R^+\right)$$

where $y^+ = y/\eta$, $\eta = \nu/u_*$ and $R^+ = (u_* R/\nu)$. Over most of the flow the appropriate scaling is the velocity deficit given by

$$\frac{U - U_c}{u_*} = F\left(\overline{y}, R^+\right)$$

where $\overline{y} = y/R$, u_* is the friction velocity and U_c is the velocity at the centerline. In the limit as $R^+ \to \infty$, these reduce to the familiar law of the wall and velocity deficit law respectively.

The fact that both these profiles describe the entire flow for finite values of R^+, but reduce to inner and outer profiles in the limit, is used to determine their functional forms in the "overlap" region which both retain. To leading order the profiles in this overlap region are given by

$$\frac{U}{u_*} = \frac{1}{\kappa} \ln y^+ + B_i$$

and

$$\frac{U - U_c}{u_*} = \frac{1}{\kappa} \ln \overline{y} + B_o$$

Unlike the classical theory, the parameters B_i, B_o, and $1/\kappa$ depend on R^+, but are asymptotically constant and satisfy the constraint

$$ln\, R^+ \frac{d(1/\kappa)}{dR^+} = -\frac{d}{dR^+}(B_i - B_o)$$

*This paper was prepared for presentation at *Disquisitiones Mechanicae* at the University of Illinois, Department of Theoretical and Applied Mechanics, Urbana, Ill, Oct 24-26, 1996.

The corresponding friction law is given by

$$\sqrt{\frac{2}{c_f}} = \frac{U_c}{u_*} = \frac{1}{\kappa} \ln R^+ + (B_i - B_o)$$

The variation of κ with R^+ is described to an excellent approximation by the semi-empirical relation

$$\frac{1}{\kappa} - \frac{1}{\kappa_\infty} = -\frac{\alpha A}{(\ln R^+)^{1+\alpha}} \tag{1}$$

where α and A must be determined from the experimental data. It follows from the constraint that

$$B_i - B_o = (B_{i\infty} - B_{o\infty}) + \frac{(1+\alpha)A}{(\ln R^+)^\alpha} \tag{2}$$

and

$$\frac{U_c}{u_*} = \frac{1}{\kappa_\infty} \ln R^+ + [B_{i\infty} - B_{o\infty}] - \frac{A}{(\ln R^+)^\alpha} \tag{3}$$

The experimental data from the superpipe experiment are carefully examined and shown to be in near perfect agreement with the new theory. The asymptotic values of the paremeters are given by $B_{i\infty} = 6.5$, $B_{o\infty} = -1.95$, and $\kappa_\infty = 0.447$, while those describing the Reynolds number dependence are given by $A = -0.668$, $\alpha = 0.44$. Thus the last term in the friction relation dies off very slowly with Reynolds number, and is negligible only when $R^+ >> 10^5$. It is interesting that the value of α is almost identical to that which arises in a similar term for a power law description of the turbulent boundary layer.

Finally, it is suggested that there exists a *mesolayer* in the region approximately defined by $30 < y^+ < 300$ in which the energy dissipation evolves from $\nu q^2/y^2$ to q^3/y. Thus the Reynolds stress and mean flow equations retain a Reynolds number dependence, even though the terms explicitly containing the viscosity are negligible. A simple turbulence model suggests that a term $C_{mi} y^{+-1}$ should be added to the overlap velocity profile to account for this effect. Because of the mesolayer, the overlap solution is clearly evident only beyond $y^+ > 300$, well outside where it has commonly been sought.

Contents

1 Introduction

Pipe and channel flows have recently become the subject of intense scrutiny, thanks in part to new experimental data which has become available from the superpipe experiment at Princeton (Zagarola and Smits 1996, Zagarola 1996). In spite of the facts that the scaling laws were established for pipes and channels more than 80 years ago (Stanton and Pannell 1914, Prandtl 1932) and that the now classical theory of Millikan was offered in 1938 for the friction law and velocity profiles, the subject has remained of considerable interest. Examples from the last 30 years alone include the analyses of Tennekes (1968), Bush and Fendell (1974), Long and Chen (1981), and Panton (1990). All of these were essentially refinements on the original Millikan theory in which the essential functional form of the friction and velocity laws was logarithmic, and only the infinite Reynolds number state was considered.

Recently Barenblatt 1978, 1993 has suggested that the velocity profiles of pipe, channel and boundary layer flows were power laws. George and his coworkers (George and Bower 1988, George 1990, 1994, George and Castillo 1993, George et al. 1993) have argued that both the velocity and friction laws for boundary layers are power laws, but that pipes and channels are logaritmic. Their work on boundary layers has recently been summarized in George et al 1996. Specifically, using the averaged equations and an Asymptotic Invariance Principle, they deduced that the proper scaling velocity for the outer part of the boundary layer was U_∞ but the inner region was scaled by u_*. The velocity profiles in the Reynolds number dependent overlap region were derived as

$$\frac{U}{u_*} = C_i \left(\frac{y}{\eta}\right)^\gamma \tag{4}$$

and

$$\frac{U - U_\infty}{U_\infty} = C_o \left(\frac{y}{\delta}\right)^\gamma \tag{5}$$

where $\eta = \nu/u_*$ and where C_i, C_o, and γ were functions of δ^+, asymptotically constant, and satisfied the constraint equation,

$$\ln \delta^+ \frac{d\gamma}{d\delta^+} = \frac{d \ln C_o/C_i}{d\delta^+} \tag{6}$$

where $\delta^+ = u_*\delta/\nu$. The friction law was given by

$$\frac{u_*}{U_\infty} = \frac{C_o}{C_i}\delta^{+-\gamma} \tag{7}$$

The Reynolds number dependence of the parameters was established using the necessary conditions for similarity and experimental data. In particular,

$$\ln C_o/C_i = (\gamma - \gamma_\infty) \ln \delta^+ + h \tag{8}$$

and

$$\gamma - \gamma_\infty = -\frac{dh}{d \ln \delta^+} \tag{9}$$

where the best choice for $h = h(\delta^+)$ was given by

$$h(\delta^+) = \frac{A}{(\ln \delta^+)^\alpha} + h_\infty \tag{10}$$

The values for the constants were determined from the data to be $\gamma_\infty = 0.0362$, $C_{o\infty}/C_{i\infty} = \exp(h_\infty) = 0.0164$, $C_o \approx C_{o\infty} = 0.897$, $A = -2.91$, and $\alpha = 0.46$. The theory was in excellent agreement with the boundary layer data, once the effects of the mesolayer (described later) were accounted for.

The purpose of this paper is to apply the same methodology to pipe and channel flows, and to compare the theory with the new experimental data. The important difference from the other efforts mentioned above is that the effects of finite Reynolds number are explicitly included.

2 Scaling Laws for Turbulent Pipe and Channel Flow

The streamwise momentum equation for a fully developed two-dimensional channel flow at high Reynolds number reduces to

$$0 = -\frac{1}{\rho}\frac{dP}{dx} + \frac{\partial}{\partial y}\left[- < uv > +\nu \frac{\partial U}{\partial y}\right] \tag{11}$$

Like the boundary layer, the viscous term is negligible everywhere but very near the wall, so that the core (or outer) flow in the limit of infinite Reynolds number is governed by

$$0 = -\frac{1}{\rho}\frac{dP}{dx} + \frac{\partial}{\partial y} - < uv > \tag{12}$$

In the limit of infinite Reynolds number, the inner layer is governed by

$$0 = \frac{\partial}{\partial y}\left[- < uv > +\nu \frac{\partial U}{\partial y}\right] \tag{13}$$

This can be integrated from the wall to obtain

$$u_*^2 = - < uv > + \nu \frac{\partial U}{\partial y} \tag{14}$$

where u_* is the friction velocity. It is obvious that the inner profiles must scale with u_* and ν since these are the only parameters in the inner equations and boundary conditions. Hence, there must be a law of the wall (at least for a limited region very close to the wall).

Because there is no imposed condition on the velocity, except at the wall, an outer scaling velocity must be sought from the parameters in the outer equation itself. Since there are only two, $-(1/\rho)dP/dx$, the externally imposed pressure gradient, and R the channel half-width, only a single velocity can be formed; namely,

$$U_o = \left(-\frac{R}{\rho} \frac{dP}{dx} \right)^{1/2} \tag{15}$$

Unlike the developing boundary layer, the channel flow is homogeneous in the streamwise direction, so there is an exact balance between the wall shear stress acting on the walls, and the net pressure force acting across the flow. This equilibrium requires that

$$u_*^2 = -\frac{R}{\rho} \frac{dP}{dx} \tag{16}$$

which is just the square of equation 15 above ; thus, $U_o = u_*$. Therefore, the outer scale velocity is also u_*, and the outer and inner velocity scales are the same. Thus channel and pipe flows are fundamentally different from boundary layer flows where asymptotic Reynolds number independence demands that the inner and outer scales for the mean velocity be different (George et al 1993).

It is obvious that since the length scales governing the inner and outer equations are different, no single scaling law should be able to collapse data for the entire flow. Moreover, since the neglected terms in both the inner and outer equations above depend on the ratio of length scales (v. Tennekes and Lumley 1972), then neither set of scaling parameters will be able to perfectly collapse the data in either region at finite values of $R^+ = Ru_*/\nu$. The Asymptotic Invariance Principle of George 1994 states that the appropriate choices for scaling are those which lead to similarity solutions of the inner and outer equations separately in the limit for which those equations themselves are valid, namely $R^+ \to \infty$.

Thus the appropriate inner and outer scaling laws for the velocity profile are

$$\frac{U}{u_*} = f_i(y^+, R^+) \tag{17}$$

and

$$\frac{U - U_c}{u_*} = f_o(\overline{y}, R^+) \tag{18}$$

where the outer velocity has been referenced to the velocity at the centerline, U_c, to avoid the necessity of accounting for the change over the inner layer. The only other difference from the boundary layer is that the outer length scale is some measure of the width of the channel, say the half-width (or pipe radius), R. Note that both of these describe the *entire* velocity profile as long as $R^+ = u_* R/\nu$, the ratio of outer to inner length scales, is retained. This is because they represent the same solutions of the complete governing equations for given R^+, but have been simply scaled differently.

If the scaled profiles above are indeed proper scaling laws, then they should by the Asymptotic Invariance Principle (AIP) become asymptotically independent of R^+ in the limit of infinite Reynolds number; i.e.,

$$\begin{aligned} \lim f_i(y^+, R^+) &\rightarrow f_{i\infty}(y^+) \\ \lim f_o(\overline{y}, R^+) &\rightarrow f_{o\infty}(\overline{y}) \end{aligned}$$

as $R^+ \rightarrow \infty$. In fact, these limiting profiles should be solutions to the inner and outer equations respectively, which are themselves valid only in the infinite Reynolds number limit.

Figures 1 and 2 show the mean velocity profile data from the superpipe experiment (Zagarola 1996, see also Zagarola and Smits 1996) in both inner and outer variables. Note the excellent collapse very close to the wall $y^+ < 10$ in inner variables and over the core region ($\overline{y} > 0.1$). Note also that the region of approximate collapse in inner variables (Figure 1) increases from the wall with increasing Reynolds number, as does the inward extent of the outer variable collapse (Figure 2).

Unlike most boundary layer measurements, the shear stress for the superpipe data has been independently determined from the pressure gradient. The close proximity of the data near the wall to the exact solution valid there ($u^+ = y^+$) gives considerable credibility to the velocity measurements, even without correction. The direct determination of the shear stress from the pressure drop down the pipe (without choosing it to collapse the 'log' layer which can only be assumed to collapse) is especially important since there is some evidence of a lack of complete collapse of the data in Figure 1 outside of $y^+ = 10$, especially for the lowest Reynolds numbers. The lack of collapse is even more apparent for the outer scaling in Figure 2 inside of $\overline{y} \approx 0.1$ which includes all of the overlap region discussed below.

3 The Overlap Layer: An Application of Near-Asymptotics

It is obvious that since the outer and inner profiles scale differently and the ratio of length scales is in fact the Reynolds number, then the region between the two similarity regimes cannot be Reynolds number independent, except possibly in the limit of infinite Reynolds number. The actual mean velocity profile at any finite Reynolds number, however, is the average of the instantaneous solutions to the Navier-Stokes equations and boundary conditions. And this profile, whether determined from a real flow by measurement, a DNS simulation, or not at all, exists, at least in principle, and is valid everywhere *regardless of how it is scaled.* Therefore both scaled forms of this solution, $f_i(y^+, R^+)$ and $f_o(\overline{y}, R^+)$ (equations 17 and 18 respectively), represent the velocity everywhere, at least as long as the Reynolds number is finite. In fact, the parameter R^+ uniquely labels the fanning out of the inner scaled profiles in the outer region and the outer scaled profiles near the wall in Figures 1 and 2.

Thus, f_i and f_o are quite unlike their limiting forms, $f_{i\infty}$ and $f_{o\infty}$, which are only infinite Reynolds number solutions for the inner and outer equations respectively. If f_i and f_o are considered instead of $f_{i\infty}$ and $f_{o\infty}$ (as is usually done), the problem of determining whether an overlap region exists is quite different from the usual asymptotic matching where infinite Reynolds number inner and outer solutions are extended and matched in an overlap region if one exists. Therefore, the objective here is *not* to see if f_i and f_o overlap and match them if they do. Rather, it is rather to determine *whether the fact that these scaled finite Reynolds number solutions (to the whole flow) degenerate at infinite Reynolds number in different ways* can be used to determine their functional forms in the common region they describe in the limit. The methodology outlined below (termed *Near-Asymptotics*) is an extension of Intermediate Asymptotics (v. Barenblatt 1978), and

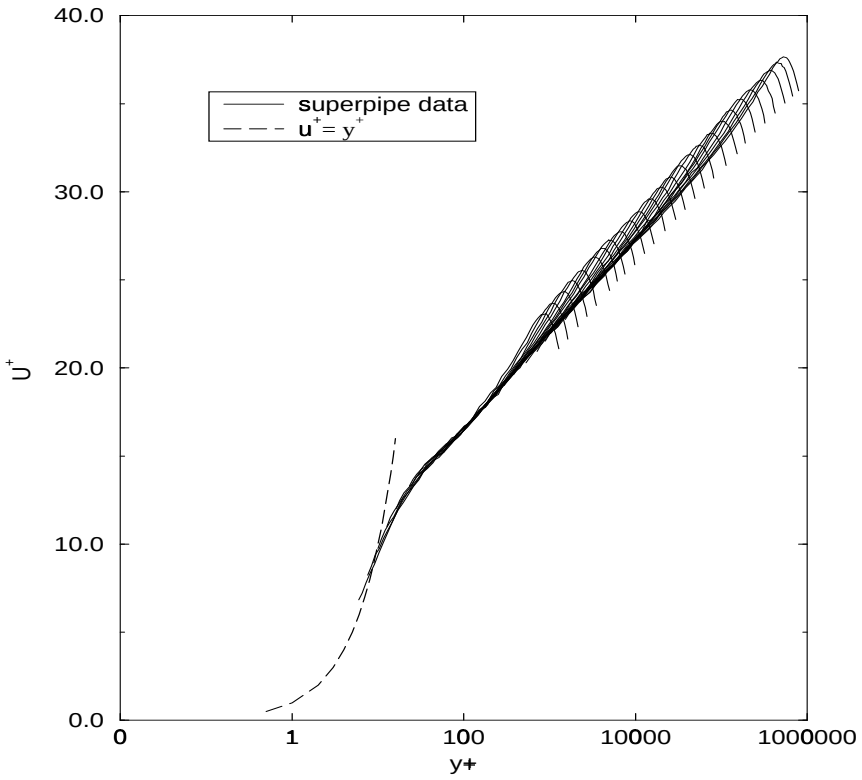

Figure 1: Velocity profiles in inner variables

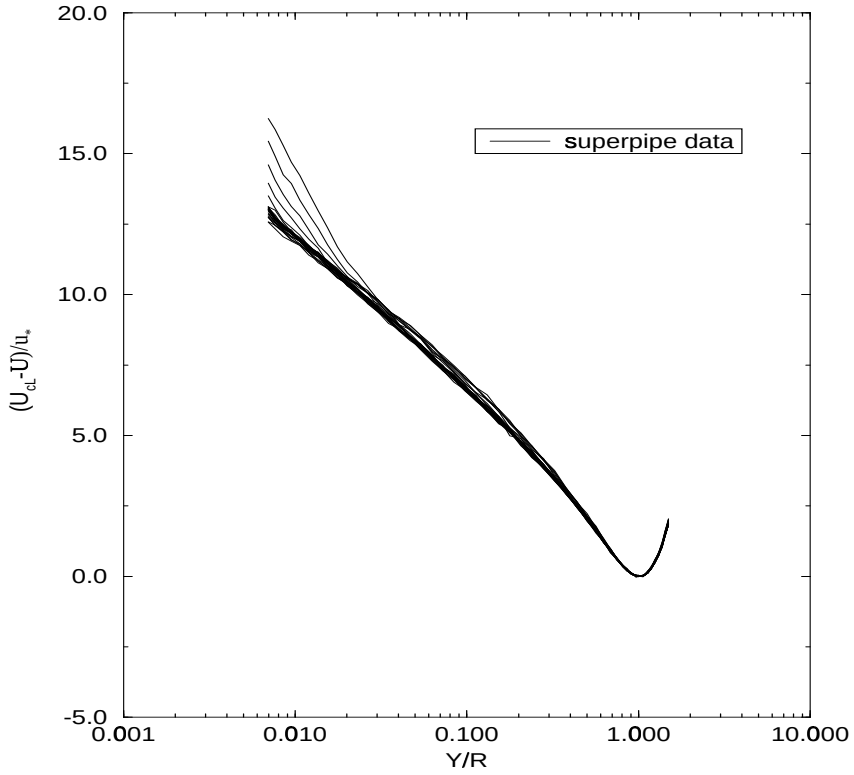

Figure 2: Velocity profiles in outer variables

is necessary because the traditional approach cannot account for the possibility of the matching parameter tending to zero, as might be the case.

The fact that analytical forms for these Reynolds number dependent solutions are not available, and they are only known *in prinicipal* turns out not to be a significant handicap. There are several pieces of information about the two profiles which can be utilized without further assumptions. They are:

- First, since both inner and outer forms of the velocity profile must describe the flow everywhere as long as the ratio of length scales, $R^+ = R/\eta$, is finite, it follows from equations 17 and 18 that

$$\frac{1}{g(R^+)} + f_o(\overline{y}, R^+) = f_i(y^+, R^+) \tag{19}$$

  where $g(R^+)$ is defined by

$$g(R^+) \equiv u_*/U_c \tag{20}$$

- Second, for finite values of R^+, the velocity derivatives from both inner and outer forms of the velocity must also be the same everywhere. It is easy to show that this implies that

$$\overline{y}\frac{\partial f_o}{\partial \overline{y}} = y^+\frac{\partial f_i}{\partial y^+} \tag{21}$$

  for all values of R^+ and y.

- Third, as noted above, in the limit both f_o and f_i must become asymptotically independent of R^+; i.e., $f_o(\overline{y}, R^+) \rightarrow f_{o\infty}(\overline{y})$ and $f_i(y^+, R^+) \rightarrow f_{i\infty}(y^+)$ as $R^+ \rightarrow \infty$.

Now the problem is that *in the limit* as $R^+ \rightarrow \infty$, the outer form fails to account for the behaviour close to the wall while the inner fails to describe the behavior away from it. The question then is: In this limit (as well as for all finite values approaching it) does there exist an "overlap" region where equation 19 is still valid? (Note that boundary layer flows are quite different from pipe and channel flows since the overlap layer in the latter remains at fixed distance from the wall for all x because of the streamwise homogeneity, as long as the external parameters are fixed, while in the former it moves away from the wall with increasing x.)

The question of whether there is a common region of validity can be investigated by examining how rapidly f_o and f_i are changing with R^+. The relative variation of f_i and f_o with Reynolds number can be related their Taylor expansions about a fixed value of R^+; i.e.,

$$\frac{f_i(y^+; R^+ + \Delta R^+) - f_i(y^+; R^+)}{\Delta R^+ f_i(y^+, R^+)} \approx \frac{1}{f_i(y^+, R^+)}\frac{\partial f_i(y^+; R^+)}{\partial R^+}\Big|_{y^+} \equiv S_i(R^+, y^+) \tag{22}$$

and

$$\frac{f_o(\overline{y}; R^+ + \Delta R^+) - f_o(\overline{y}; R^+)}{\Delta R^+ f_o(\overline{y}, R^+)} \approx \frac{1}{f_o(\overline{y}, R^+)}\frac{\partial f_o(\overline{y}; R^+)}{\partial R^+}\Big|_{\overline{y}} \equiv S_o(R^+, \overline{y}) \tag{23}$$

Thus S_i and S_o are a measure of the Reynolds number dependences of f_i and f_o respectively. Both vanish identically in the limit as $R^+ \rightarrow \infty$. If ${y^+}_{max}$ denotes a location where outer flow effects begin to be strongly felt on the inner scaled profile, then for $y^+ < {y^+}_{max}$, S_i should be much less than unity (or else the inner scaling is not very useful). Similarly, if $\overline{y}_{min}$ measures the location where viscous effects begin to be strongly

felt (e.g., as the linear velocity region near the wall is approached), then S_o should be small for $\overline{y} > \overline{y}_{min}$. Obviously either S_i or S_o should increase as these limits are approached. Outside these limits, one or the other should increase dramatically.

The quantities S_i and S_o can, in fact, be used to provide a formal definition of an "overlap" region where both scaling laws are valid. Since S_i will increase drastically for large values of y for given R^+ and S_o will increase for small values of y, an "overlap" region exists only if there exists a region for which both S_i and S_o remain small simultaneously. In the following paragraphs, this condition will be used in conjunction with equation 19 to derive the functional form of the velocity in the overlap region *at finite Reynolds number*, hence the term 'Near-Asymptotics'. This is, of course, Intermediate Asymptotics, but at finite Reynolds numbers.

Because of the movement of the matched layer toward the wall with increasing R^+, it is convenient and necessary to introduce an intermediate variable $\tilde{y}$ which can be fixed in the overlap region all the way to the limit, regardless of what is happening in physical space (v. Cole and Kevorkian 1981). A definition of $\tilde{y}$ which accomplishes this is given by

$$\tilde{y} = y^+ {R^+}^{-n} \tag{24}$$

or

$$y^+ = \tilde{y} {R^+}^{n} \tag{25}$$

Since $\overline{y} = y^+/R^+$, it follows that

$$\overline{y} = \tilde{y} {R^+}^{n-1} \tag{26}$$

For all values of n satisfying $0 < n < 1$, $\tilde{y}$ can remain fixed in the limit as $R^+ \to \infty$ while $\overline{y} \to 0$ and $y^+ \to \infty$. Substituting these into equation 19 yields the matching condition on the velocity in terms of the intermediate variable as

$$\frac{1}{g(R^+)} + f_o({R^+}^{n-1}\tilde{y}, R^+) = f_i({R^+}^{n}\tilde{y}, R^+) \tag{27}$$

Now equation 27 can be differentiated with respect to R^+ *for fixed* $\tilde{y}$ to yield equations which explicitly include S_i and S_o. The result after some manipulation is

$$\overline{y}\left(\frac{\partial f_o}{\partial \overline{y}}\right)_{R^+} = \frac{1}{\kappa} - R^+[S_i(y^+, R^+)f_i(y^+, R^+) - S_o(\overline{y}, R^+)f_o(\overline{y}, R^+)] \tag{28}$$

where

$$\frac{1}{\kappa(R^+)} \equiv -\frac{R^+}{g^2}\frac{dg}{dR^+} = \frac{d(1/g)}{d\ln R^+} \tag{29}$$

Note that the first term on the right hand side 28 is at most a function of R^+ alone, while the second term contains all of the residual y-dependence.

Now it is clear that if both

$$R^+|S_o|f_o << 1/\kappa \tag{30}$$

and

$$R^+|S_i|f_i << 1/\kappa \tag{31}$$

then the first term on the right-hand side of equation 28 dominates. If $1/\kappa \to 0$, then the inequalities are still satisfied as long as the left hand side does so more rapidly than $1/\kappa$. Note that a much weaker condition

can be applied which yields the same result; namely that both inner and outer scaled profiles have the same dependence on R^+, i.e., $S_i f_i = S_o f_o$ in the overlap range so $1/\kappa$ is the only term remaining. If these inequalities are satisfied over some range in y, then to leading order, equation 28 can be written as

$$\overline{y}\frac{\partial f_o}{\partial \overline{y}} = \frac{1}{\kappa} \tag{32}$$

The solution to equation 32 can be denoted as $f_o^{(1)}$ since it represents a first order approximations to f_o. It is *not*, however, simply the same as $f_{o\infty}$ because of the R^+ dependence of $1/\kappa$, but reduces to it in the limit. Thus, by regrouping into the leading term all of the y-independent contributions, the method applied here has yielded a more general result than the customary expansion about infinite Reynols number. (It is also easy to see why the usual matching of infinite Reynolds number inner and outer solutions will not work if the limiting value of $1/\kappa$ is zero.)

From equations 21 and 32, it follows that

$$y^+\frac{\partial f_i}{\partial y^+} = \frac{1}{\kappa} \tag{33}$$

An interesting feature of these first order solutions is that the inequalities given by equations 30 and 31 determine the limits of validity of both equations 32 and 33 since either S_o or S_i will be large outside the overlap region. Clearly the extent of this region will increase as the Reynolds number (or R^+) increases.

Equations 32 and 33 can be readily integrated to yield (to leading order)

$$f_o^{(1)}(\overline{y}, R^+) = \frac{1}{\kappa(R^+)} ln\overline{y} + B_o(R^+) \tag{34}$$

and

$$f_i^{(1)}(y^+, R^+) = \frac{1}{\kappa(R^+)} lny^+ + B_i(R^+) \tag{35}$$

In the remainder of this paper, the superscript '(1)' will be dropped; however it is these first order solutions that are being referred to unless otherwise stated. Thus the velocity profiles in the overlap are logarithmic, but with parameters which are Reynolds number dependent.

The parameters $1/\kappa$, B_i and B_o must themselves be asymptotically constant since since the equations to which they are solutions are themselves Reynolds number independent in the limit (the AIP). Moreover, the limiting values, κ_∞, $B_{i\infty}$, and $B_{o\infty}$ cannot all be zero, or else the solutions themselves are trivial. In fact, since in the limit of infinite Reynolds number the energy balance in the overlap range reduces to production equals dissipation (i.e.,

$$\epsilon^+ = du^+/dyi) = (\frac{1}{\kappa y^+}) \tag{36}$$

and the energy dissipation rate must be finite and non-zero, it follows that $1/\kappa_\infty$ must be finite and non-zero. It will be shown below that these conditions severely restrict the possible Reynolds number dependencies for the parameters.

The relation between u_* and U_c follows immediately from equation 19; i.e.,

$$\frac{1}{g(R^+)} = \frac{1}{\kappa(R^+)} lnR^+ + [B_i(R^+) - B_o(R^+)] \tag{37}$$

Thus the friction law is entirely determined by the velocity parameters for the overlap region. However, equation 29 must also be satisfied. Substituting equation 37 into equation 29 implies that κ, B_i, and B_o are constrained by

$$lnR^+ \frac{d(1/\kappa)}{dR^+} = -\frac{d(B_i - B_o)}{dR^+} \tag{38}$$

Equation 38 is exactly the criterion for the neglected terms in equation 28 to vanish identically (i.e., $S_i f_i - S_o f_o \equiv 0$). Therefore the solution represented by equations 34 – 38 is, indeed, the first order solution for the velocity profile in the overlap layer at *finite*, but large, Reynolds number. Clearly when y^+ is too big or $\overline{y}$ is too small for a given value of R^+, the inequalities of equation 30 and 31 cannot be satisfied. Since all the derivatives with respect to R^+ must vanish as $R^+ \to \infty$ (the A.I.P.), the inner range of the outer overlap solution is unbounded in the limit, as is the outer range of the inner.

Thus the velocity profile in the overlap layer is logarithmic, *but* with parameters coefficients and exponent which depend on Reynolds number, R^+. The functions $\kappa(R^+)$, $B_i(R^+)$ and $B_o(R^+)$ must be determined either empirically or from a closure model for the turbulence. Regardless of how they are determined, the results must be consistent with equation 38.

4 A Solution for the Reynolds Number Dependence

It is convenient to transform equation 38 using

$$H(R^+) = \left(\frac{1}{\kappa} - \frac{1}{\kappa_\infty}\right) \ln R^+ + (B_i - B_o) \tag{39}$$

where $H = H(R^+)$ remains to be determined. It is easy to show that if $H(R^+)$ satisfies

$$\frac{1}{\kappa} - \frac{1}{\kappa_\infty} = \frac{dH}{d \ln R^+} \tag{40}$$

then equation 38 is satisfied. It follows immediately that

$$\frac{1}{g} = \frac{U_c}{u_*} = \frac{1}{\kappa_\infty} \ln R^+ + H(R^+) \tag{41}$$

Thus the Reynolds number dependence of $H(R^+)$ determines that of both κ and $B_i - B_o$.

It is easy to show that the condition that both $B_{i\infty}$ and $B_{o\infty}$ be finite and non-zero requires that:

- *Either* B_i, B_o and κ remain constant always;

or

- (i) $1/\kappa \to 1/\kappa_\infty$ faster than $1/\ln R^+$, and
- (ii) $H(R^+) \to H_\infty = constant$.

Obviously from equation 39,

$$H_\infty = B_{i\infty} - B_{o\infty} \tag{42}$$

An empirical choice for $H(R^+) - H_\infty$ satisfying these conditions is suggested by the boundary layer analysis of George et al (1993); it is,

$$H(R+) - H_\infty = \frac{A}{[\ln R^+]^\alpha} \tag{43}$$

Note that conditions (i) and (ii) above imply that $\alpha > 0$.

Using this in equation 41 yields

$$\frac{U_c}{u_*} = \frac{1}{\kappa_\infty} \ln R^+ + [B_{i\infty} - B_{o\infty}] + \frac{A}{[\ln R^+]^\alpha} \tag{44}$$

Note that as $R^+ \to \infty$ this reduces to the classical solution of Millikan 1938.

The Reynolds number variationn of $1/\kappa$ and $B_i - B_o$ can be immediately obtained from equations 39, 40 and 43 as

$$\frac{1}{\kappa} - \frac{1}{\kappa_\infty} = \frac{-\alpha A}{(\ln R^+)^{1+\alpha}} \tag{45}$$

and

$$(B_i - B_o) - (B_{i\infty} - B_{o\infty}) = \frac{(1+\alpha)A}{(\ln R^+)^\alpha} \tag{46}$$

Figures 3a and 3b show the friction data of the superpipe experiment of Zagarola and Smits (1996). Careful scrutiny reveals that the data do not fall on a straight line, so a simple logarithmic friction law with constant coefficients does not describe all the data. Figure 3b also shows two curves: The first represents a regression fit of equation 44 (also shown on Figure 3a), while the second shows only the asymptotic log form of equation 44.

The former provides an excellent fit to the data for *all* Reynolds numbers and asymptotes exactly to the latter, but only at much higher Reynolds numbers. The differences although slight are very important since they entirely determine (or reflect) the Reynolds number dependence of the parameters $1/\kappa$, B_i and B_o. The latter will be seen later to be especially sensitive to this dependence.

The values obtained for the friction law parameters are $\kappa_\infty = 0.447$, $B_{i\infty} - B_{o\infty} = 8.45$, while those describing the Reynolds number dependence are $A = -0.668$ and $\alpha = 0.441$. Note that the values of $B_{i\infty}$ and $B_{o\infty}$ cannot be determined individually from the friction data, only their difference. The values of κ_∞ and $B_{i\infty} - B_{o\infty}$ differ only slightly from the values determined by Zagarola (1996) (0.44 and 7.8) using the velocity profiles alone and assuming that the asymptotic state had been reached. All the parameters are remarkably independent of the particular range of data utilized. For example, of the 26 different Reynolds numbers available, the highest 15 Reyolds numbers could be dropped before even changing the second digit of the values of the parameters cited above. This suggests strongly that the data are in fact a smooth curve, uncontaminated by roughness, and that the proposed form of H properly captures the shape of the Reynolds number dependence.

For the boundary layer the friction data were not as reliable as those reported here, so that the functional form of H had to be inferred after a variety of attempts to describe the variation of the exponent in a power law description of the velocity profile in the overlap region. Interestingly, the value for α obtained here is almost exactly the value obtained for the boundary layer data (0.461 versus 0.44). In view of the differing definitions of the length scales, the physical significance of this, if any, is not yet clear.

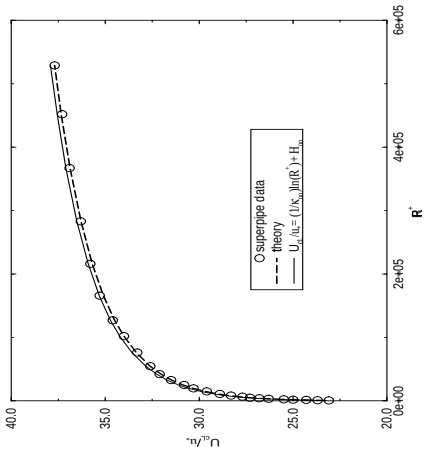

(1) (2)

Figure 3: Variation of U_c/u_* with $R^+ = Ru_*/\nu$

5 The Effect of Reynolds Number on the Overlap Range

The parameters established for the friction law will be used below to calculate the values of κ, B_i and B_o for each Reynolds number of the superpipe data. Only either of the B's need be established from the experiments since their difference is known from equation 39. Before carrying out a detailed comparison with the velocity data, however, it is is useful to first consider exactly which region of the flow is being described by the overlap profiles. Also of interest is the question of how large the Reynolds number must be before the flow begins to show the characteristics of the asymptotic state.

The overlap layer identified in the preceding sections can be related directly to the averaged equations for the mean flow and the Reynolds stresses. From about $y^+ > 10 - -20$ approximately, out to about the center of the flow, the averaged momentum equation is given approximately by

$$0 = -\frac{\partial < uv >}{\partial y} - \frac{1}{\rho}\frac{dP}{dx} \tag{47}$$

It has no explicit Reynolds number dependence; and the Reynolds shear stress is drops linearly all the way to the center of the flow. Inside about $\overline{y} = 0.1$, however, the Reynolds shear stress is nearly constant. In fact, at infinite Reynolds number the pressure gradient term vanishes identically and the mean momentum equation reduces to

$$0 = -\frac{\partial < uv >}{\partial y} \tag{48}$$

At finite (but large) Reynolds numbers this region is similar to the developing boundary layer where the Reynolds stress is effectively constant. Obviously it it reasonable to expect the overlap region to more or less correspond to this constant stress layer. (Note that many low Reynolds number boundary layer experiments do not have a region where this is even approximately true because the convection terms are not truly negligible. Hence it is unreasonable to expect such experimental profiles to display any of the characteristics of the overlap described above, except possibly in combination with the characteristics of the other regions.)

Even when there is a region of reasonably constant Reynolds stress, however, this is not the entire story because of the Reynolds number dependence of $- < uv >$ itself. And it is this weak Reynolds number dependence which is the reason that κ, B_i, and B_o are only asymptotically constant. The origin of this weak Reynolds number dependence (which is well-known to turbulence modellers) can be seen by considering the Reynolds transport equations. For the same region, $y^+ > 10 - -20$, the viscous diffusion terms are negligible (as in the mean momentum equation), so the equations reduce approximately to (Tennekes and Lumley 1972),

$$0 = -(< p\frac{\partial u_i}{\partial x_k} > + < p\frac{\partial u_k}{\partial x_i} >) - \left[< u_i u_2 > \frac{\partial U_k}{\partial x_2} + < u_k u_2 > \frac{\partial U_i}{\partial x_2}\right] - \frac{\partial < u_i u_k u_2 >}{\partial x_2} - \epsilon_{ik} \tag{49}$$

where $U_i = U\delta_{i1}$. Thus viscosity does not appear directly in any of the single point equations governing this region, nor does it appear in those governing the outer boundary layer.

In spite of the above, however, viscosity can be shown to play a crucial role in at least a portion of the constant stress layer, even at infinite Reynolds number. The reason is that the *scales of motion* at which the dissipation, ϵ_{ik}, actually takes place depend on the *local* turbulence Reynolds number, $R_t = q^4/\nu\epsilon$. For $R_t > 1000$ approximately, the energy dissipation is nearly completely controlled by the large energetic scales of motion. These are effectively inviscid, but control the energy transfer through non-linear interactions (the

energy cascade) to the much smaller viscous scales where the actual dissipation occurs (v. Tennekes and Lumley 1972). When this is the case, the dissipation is nearly isotropic so $\epsilon_{ik} \approx 2\epsilon\delta_{ik}$. Moreover, ϵ can be approximated by the infinite Reynolds number relation: $\epsilon \sim q^3/L$ where L is a scale characteristic of the energy-containing eddies. The coefficient has a weak Reynolds number dependence, but is asymptotically constant. Thus, the Reynolds stress equations are effectively inviscid, but only exactly so in the limit. Note that in this limit the Reynolds shear stress has no dissipation at all, i.e., $\epsilon_{12} = 0$.

At very low turbulence Reynolds number, however, the dissipative and energy-containing ranges nearly overlap, and so the latter (which also produce the Reynolds shear stress) feels directly the influence of viscosity. In this limit, the energy and dissipative scales are about the same, so the dissipation is more reasonably estimated by $\epsilon \sim \nu q^2/L^2$, where the constant of proportionality is of order 10. The dissipation tensor, ϵ_{ik} is anisotropic and ϵ_{12}, in particular, is non-zero (Launder 1993). (Hanjalic and Launder 1972, for example, take $\epsilon_{12} = (- < u_1 u_2 > /q^2)\epsilon$.)

For turbulence Reynolds numbers between these two limits, the dissipation will show characteristics of both limits, gradually making a transition from $\epsilon \sim \nu q^2/L^2$ to $\epsilon \sim q^3/L$ as R_t increases. Thus the Reynolds stresses themselves will feel directly this, and will show a strong Reynolds number dependence. Obviously, in order to establish when (if at all) parts of the flow become Reynolds number independent, it is necessary to determine how the local turbulence Reynolds number varies downstream and across flow.

Over the outer boundary layer (which is most of it), $L \approx R/2$ and $q \approx 3u_*$. So when $R^+ > 7,000$, the dissipation in the outer flow is effectively inviscid. Above this value the mean and turbulence quantities in the core region of the flow should show little Reynolds number dependence, This is indeed the case as illustrated by Figure 2. The outer region can, of course, not be entirely Reynolds number independent, except in the limit, and this residual dependence manifests itself in the overlap layer in the slow variations of κ and B_o, for example.

The near wall region is considerably more interesting since in it the scales governing the energy-containing eddies are constrained by the proximity of the wall. Hence, the turbulence Reynolds number, R_t, depends on the distance from the wall, y. In fact, $R_t \sim y^+$ with a coefficient of about 3; so, in effect, y^+ is the turbulence Reynolds number. Because of this, two things are immediately obvious:

- First, as the Reynolds number increases more and more of the pipe (in outer variables) will become effectively inviscid and will be governed by the inviscid dissipation relation. And correspondingly, the mean and turbulence quantities in the overlap layer will become Reynolds number independent, albeit very slowly. Clearly these limiting values cannot be reached until the entire overlap layer is governed by the infinite Reynolds number dissipation relation and its coefficient has reached the limiting value. Obviously this can happen only when there is a substantial range satisfying $y^+ > 300$ and for which the mean convection terms are negligible, typically $\overline{y} < 0.1$. Thus the asymptotic limits are realized only when $300\nu/u_* << 0.1R$ or $R^+ >> 3000$. Therefore the overlap layer below approximately $R^+ = 30,000$ should display a Reynolds number dependence, not only in κ, B, and B_1, but correspondingly in the behavior of $< u^2 >$, $< uv >$, etc.

- Second, there will always be a *MESOLAYER* [1], below about $y^+ \approx 300$ in which the dissipation can *never* assume the character of a high Reynolds number flow, no matter how high the Reynolds number

[1] This appropriates a term from Long 1976 (see also Long and Chen 1982) who argued strongly for its existence, but from entirely different physical and scaling arguments which we find untenable. Nonetheless, despite the skepticism which greeted his ideas, Long's instincts were correct.

becomes. This is because the dissipation (and Reynolds stress as well) can never become independent of viscosity — even though the mean momentum equation itself is inviscid above $y^+ \approx 10$! This fact is well-known to turbulence modellers (v. Hanjalic and Launder 1972), but the consequences for similarity theory and asymptotic analyses do not seem to have been noticed previously. It is particularly important for experimentalists who have routinely tried to apply asymptotic formulas to data from to this region, wrongly believing the mesolayer to be the overlap region.

Thus the constant stress layer is really four separate regions, each having their own unique character. The overlap layer ($y^+ > 300$, $\overline{y} < 0.1$) obtained in the preceding section which is nearly inviscid; an 'in-between layer' or mesolayer ($10 < y^+ < 300$) in which the viscous stresses are negligible, but in which viscosity acts directly on the turbulence scales producing the Reynolds stresses; a buffer layer ($5 < y^+ < 10$) where the Reynolds stress and viscous stress both act directly on the mean flow; and the real viscous sublayer, the linear region near the wall ($y^+ < 5$) where the viscous stresses dominate. And of these four regions, the overlap layer will be the *last* to appear as the flow develops or as the Reynolds number is increased. *Thus, the overlap layer will be the most difficult to identify at the modest Reynolds numbers of most laboratory experiments.* Identification will be easier if the properties of the mesolayer are known, and accordingly a model for it is presented in the next section.

6 A Mesolayer Model

It was Long 1976 (see Long and Chen 1982) who first argued for the existence of a mesolayer — but on very different physical grounds. He did not consider the turbulence energy equation, but instead only the mean momentum equation. From it he argued that some residual viscous stress must be retained in addition to the Reynolds stress, and used this to define a meso-length scale which varied as the square root of the flow Reynolds number. All subsequent deductions were based on matching four flow regions, one of which was characterized by this new length scale. The suspicion that a new layer involving viscosity and inertia was needed between the overlap and viscous layers has proven to be quite insightful. The arguments, however, can not be justified since there is simply no physical basis for arguing that the viscous stress must be important *in the equations for the mean flow.* In fact it is negligible outside of $y^+ \approx 10$. It was argued in the preceding section that viscosity enters the dynamics of the mesolayer only through its effect on the energy cascade, and that is reflected in the nature of the dissipation, and in turn in the component Reynolds stress equations.

It is easy to show that no new length scale is necessary to account for this dissipation effect. The whole reason for the existence of this mesolayer is that the local turbulence Reynolds number near the wall can never be large enough for the dissipation to become inviscid. Near the bottom of the constant stress layer, the scales of the energy-containing eddies and those at which the energy is dissipated will be nearly the same size, and in this limit $\epsilon \sim \nu q^2/L^2$ where L is typically about equal to y, the distance from the wall. At the outer part of the constant stress layer, the required scale separation will have been achieved — if the flow Reynolds number is high enough — so the dissipation is nearly inviscid and thus $\epsilon \sim q^3/y$. The essence of the mesolayer is that neither of these limits applies and a transition from one to the other is occuring. Thus in the mesolayer, $\nu q^2/y^2 \sim q^3/y$, and it follows immediately the length scale for the mesolayer is just proportional to $y \sim \nu/q \approx \nu/u_*$. But this just says that the mesolayer length scale is proportional to the viscous one. It does show clearly, however, that the mesolayer is bounded by relatively fixed values of y^+ as argued earlier, the slight variation being due to the fact the ratio q/u_* has a weak Reynolds number dependence (for a given of y^+) and is constant only in the limit.

In the mesolayer, the nature of the dissipation is changing with distance from the wall as the local Reynolds number, y^+, increases. And it is this evolution from low to high Reynolds number dissipation which provides a clue for building a model for at least part of the mesolayer. Note that the analysis below is a *physical model* based on an assumed form of the dissipation, and is therefore quite distinct from the AIP and Near Asymptotics approach described earlier. It will be shown, however, to be consistent with the latter, and to lend considerable insight into it.

Since it is the dissipation itself which creates the mesolayer, it is reasonable to begin by assuming a form for how the dissipation changes with Reynolds number, and then pursuing its logical consequences. A simple model incorporating both the high and low Reynolds number dissipation limits is

$$\epsilon = c_1 \frac{q^3}{L} + c_2 \nu \frac{q^2}{L^2} \tag{50}$$

For very high values of qL/ν the first term dominates, but the second overwhelms it when $qL/\nu << c_2/c_1$. Variations on this idea have appeared in numerous low Reynolds number turbulence models (c.f. Hanjalic and Launder 1973, Reynolds 1976, Rodi 1993). Since only the near wall region is of interest, it is appropriate to take $L = y$, as done by many single equation turbulence modellers for the near wall region.

As long as $0.1R^+ > y^+ > 30$ approximately, the kinetic energy equation for the turbulence reduces to simply a balance between production and dissipation, the turbulence transport terms being negligible; i.e.,

$$- < uv > \frac{\partial U}{\partial y} = \epsilon \tag{51}$$

The turbulence transport terms are certainly not negligible in the region $10 < y^+ < 30$ which is also part of the mesolayer, so any success of the model in this region must be regarded as fortuitous. (The authors are grateful to Drs. M.M. Gibson and W.P. Jones of the Imperial College of London for helpful discussion about this region.)

Now consistent with the single equation turbulence model is the assumption that the Reynolds stress can be modelled with an eddy viscosity acting on the mean velocity gradient; i.e.,

$$- < uv >= \nu_t \frac{dU}{dy} \tag{52}$$

The usual choice of turbulence modellers is (Rodi 1993)

$$\nu_t = c_3^2 \frac{q^4}{\epsilon} \tag{53}$$

Substituting the dissipation and Reynolds stress models into the energy balance of equation 51, dividing by q^4/ϵ, and taking the square root yields

$$\frac{\partial U}{\partial y} = \left(\frac{c_1}{c_3}\right) \frac{q}{y} + \left(\frac{c_2}{c_3}\right) \frac{\nu}{y^2} \tag{54}$$

or in inner variables,

$$\frac{du^+}{dy^+} = \left(\frac{c_1}{c_3}\right) \left(\frac{q}{u_*}\right) y^{+-1} + \left(\frac{c_2}{c_3}\right) y^{+-2} \tag{55}$$

Obviously it is the factor q/u_* which determines whether the first term on the right hand side integrates to a logarithm or a power law (or something else). For boundary layer flows, George et al. 1996 have shown this to depend on a power of y^+, consistent with the power law velocity profile. Pipe and channel flows, however, show a logarithmic dependence for all quantities. If the additive constant in the logarithm dominates so that q/u_* itself is nearly constant, then the first term yields the logarithmic overlap profile derived earlier *plus* an additional term due to the low local Reynolds number; i.e.,

$$u^+ = [\frac{1}{\kappa}\ln + B_i] + C_{mi}y^{+^{-1}} \tag{56}$$

where the parameters c_1, c_2 and c_3 have been collected into $1/\kappa$, B_i and C_{mi}. Note that the second term is unaffected by the behavior of q/u_*; hence there is reason to hope that it may be the same for all wall-bounded flows. (Note that equation 56 can also be derived using only the overlap characteristics without reference to an eddy viscosity model.)

Thus the additional contribution of the mesolayer to the velocity profile (in inner variables) is $C_{mi}y^{+^{-1}}$. The parameter C_{mi} must be negative and should be nearly constant. For the boundary layer profiles it appears that this is indeed the case and $C_{mi} \approx -37$. This value will be used in the next section without any attempt to optimize it for the pipe flow data. It is important to note that because of the relative values of B_i and C_{mi}, there is no region where the second term dominates, at least where the assumptions are valid. Therefore there will be no $y^{+^{-1}}$-layer, only a modified log region. Moreover, because of this, the first term in equation 56 will be clearly visible only when the second is negligible. Since this is not the case for many of the low and moderate Reynolds number experiments, it will not be possible to even identify the parameters B_i, B_o, and κ for most of the data *without first accounting for the mesolayer contribution.*

Equation 56 can be expressed in outer variables as

$$\frac{U - U_c}{u_*} = \frac{1}{\kappa}\ln R^+ + B_o + \frac{C_{mo}}{\overline{y}} \tag{57}$$

where

$$C_{mo} = C_{mi}R^{+^{-1}} \tag{58}$$

Obviously if C_{mi} is constant, C_{mo} is not.

Before leaving this section it might be noted that it should be possible to calculate values for the parameters using the values for c_1, c_2 and c_3 from the many turbulence models which have determined them. Unfortunately, all have been chosen to conform to the old log law, and at distances from the wall which are well inside the mesolayer defined here (eg. Reynolds 1976). If the above arguments are indeed correct, then these model constants should be re-evaluated.

7 The Velocity Data

Now that the approximate region of validity of the overlap solution has been established as $300 < y^+ < 0.1R^+$ it is possible to test the theoretical profiles and the proposed model for the Reynolds number dependence. If they are correct, only an independent determination of either B_i or B_o is necessary to completely specify the profile, the rest of the parameters having been determined from the friction data. Also it should be possible to determine whether the proposed mesolayer model is reasonable, at least for those data sets where data are available below $y^+ = 300$.

For all of the data sets it appears $B_i = 6.50$ is nearly optimal (at least for values of $R^+ < 850$, the lowest available from the superpipe experiment), so that for the remainder of this paper it will be assumed that $B_i = B_{i\infty}$. This value is very close to the value of 6.3 determined by Zagarola and Smits (1996a) by assuming κ fixed at 0.44. Since the difference, $B_{i\infty} - B_{o\infty} = 8.45$, was established from the friction data, it follows immediately that $B_{o\infty} = -1.95$.

The constancy of B_i implies that it is B_o which shows all the Reynolds number dependence of the difference given by equation 46. Figures 4 and 5 show the theoretical variation of $1/\kappa$ and B_o with Reynolds number (equations 39 and 40. Clearly both converge very slowly to their asymptotic values. This slow approach has far more relative effect on B_o than it does on $1/\kappa$, however, since B_o has achieved only 85% of its asymptotic value at $R^+ = 10^5$. The observed variation of $1/\kappa$ and B_o and the constancy of B_i can be contrasted with the boundary layer results of George et al 1996 in which C_o, the outer coefficient was nearly constant while the power exponent γ and the inner coefficient C_i varied over the entire range of Reynolds numbers available.

The relative behavior of B_o and B_i means that the outer profile scaling shows more variation with Reynolds number in the overlap region than does the inner where only κ varies. This undoubtedly explains a great deal of the problems historically in establishing what $B_{o\infty}$ is and in determining whether the outer scaling is correct. And it might also explain the conclusion of Zagarola and Smits (1996) that a different scale for the outer flow is required, especially if attention is focussed on the overlap region instead of the core region of the flow.

of the superpipe data in inner and outer variables respectively, together with the overlap solution using equations 34 and 35 and the model equations 45 and 46. The vertical lines on each profile show the suggested bounds for the mesolayer model ($30 < y^+ < 300$ or $30/R^+ < \overline{y} < 300/R^+$) and the overlap region ($300 < y^+ < 0.1R^+$ or $300/R^+ < \overline{y} < 0.1$). Note that because of the varying Reynolds number, the limits depending on R^+ are different for each profile. As noted above, the boundary layer value for the mesolayer parameter of $C_{mi} = -37$ was used.

The overlap plus mesolayer solution provides an excellent fit to the data from $70 < y^+ < 0.1R^+$ for the entire range of Reynolds numbers available. The mesolayer term captures well the point of departure from the overlap solution, as well as the deviations from it below $y^+ = 300$, even for the lowest Reynolds number where there is no overlap region at all. It does not, however, describe the profile down to $y^+ = 30$ as expected, since the velocity data bend away from the overlap plus mesolayer solution back to the overlap solution alone below about $y^+ = 80 - 90$. This may indicate that the lower limit on the proposed mesolayer model is higher than believed, or it may simply represent a problem with the data used here which were not corrected for the various sources of error near the peak in the turbulence intensity (Smits, private communication). The corrections which were applied by Zagarola (1996) to some of the data were primarily important below $y^+ = 100$ and move the data close to the mesolayer/overlap result. The excellent agreement for $100 < y^+ < 300$, however, suggests that both the form of the mesolayer model and the boundary layer value for C_{mi} are essentially correct. The agreement between experiment and theory is particularly gratifying in view of the fact that the velocity data were only used to establish B_i, the remaining parameters having been entirely determined by the friction data.

It is easy to see how the deviations from the log law due to the mesolayer could be viewed as a separate and distinct region. For example, Zagarola and Smits (1996) argue that the region $50 < y^+ < 500$ is described by a 1/7 power law with a coefficient of 8.7, and not the logarithmic profile (with constant coefficients) which fits the inner solution between $500 < y^+ < 0.1R^+$. If a power law is fitted to data generated by the overlap plus mesolayer profile proposed herein using the constants determined above, it produces almost exactly the

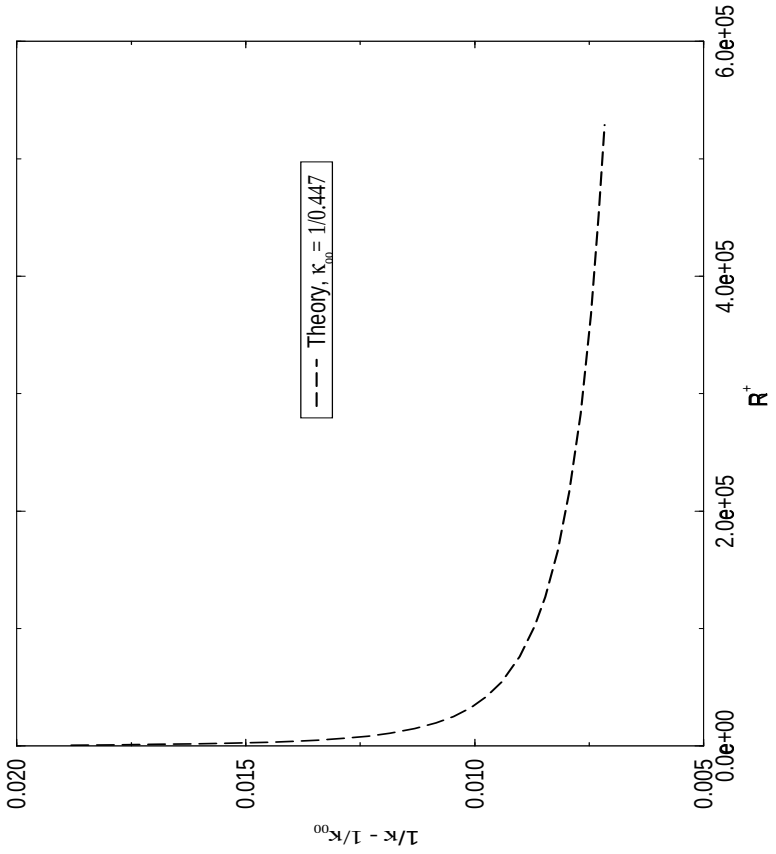

Figure 4: Variation of $1/\kappa - 1/\kappa_\infty$ with R^+, $\kappa_\infty = 0.447$

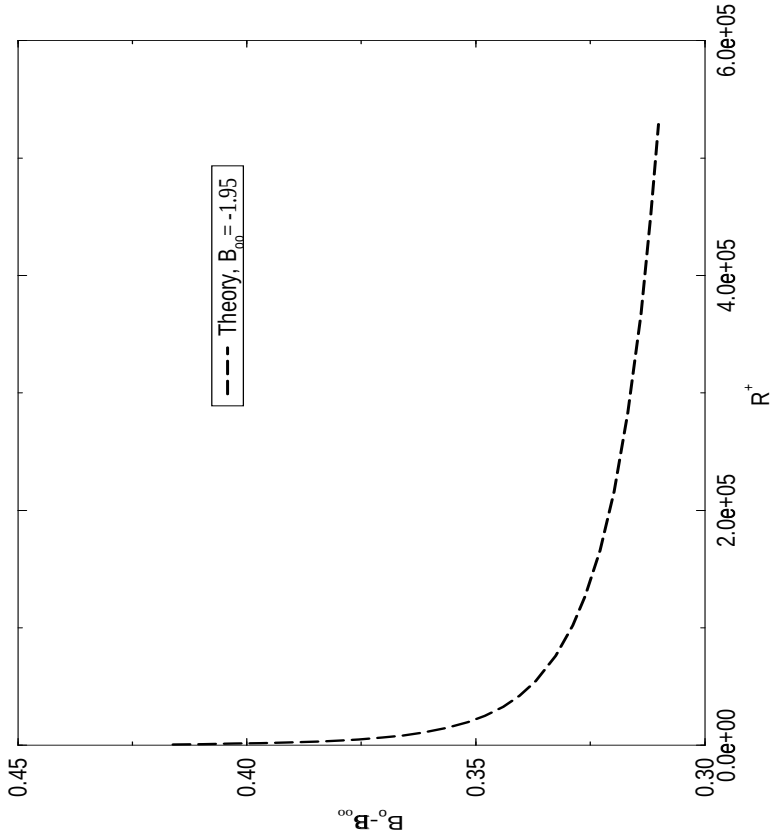

Figure 5: Variation of $B_o - B_{o\infty}$ with R^+, $B_{o\infty} = 8.50$

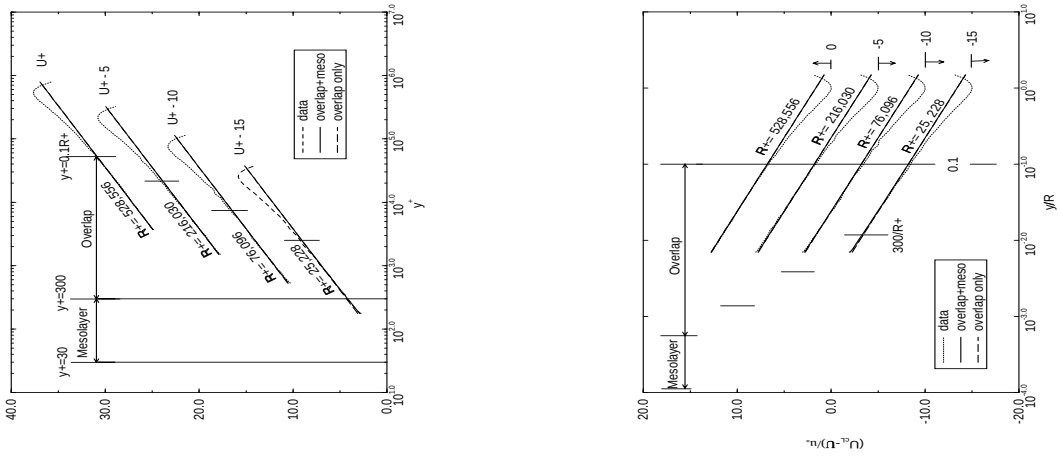

(1) (2)

Figure 6: Inner and outer profiles at relatively low Reynolds number

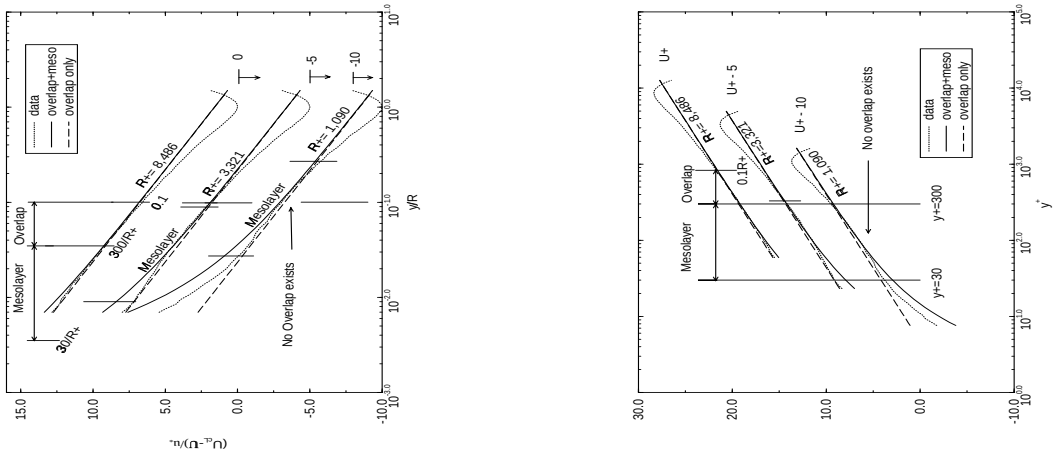

(1) (2)

Figure 7: Inner and outer profiles at relatively high Reynolds number

same 1/7-power and 8.7 coefficient over the same range. Thus it is clear that the same phenomenon is being described.

8 Summary and Conclusions

The Asymptotic Invariance Principle, the deductions from Near-Asymptotics, and the Mesolayer model have provided an excellent description of the entire range of data for the superpipe experiment from $30 < y^+ < 0.1R^+$. Of the six parameters needed to describe the flow, four had to be determined from the data ($\kappa_\infty = 0.447$, $B_{i\infty} = 6.5$, $B_{o\infty} = -1.95$, and $A = -0.668$), and are probably unique to pipe flow. The mesolayer parameter, $C_{mi} = -37$ and the parameter describing the Reynolds number dependence, $\alpha = 0.44$, appear to be the same as for the boundary layer. The possible universality of the latter two is particularly interesting, especially given the agreement between theory and experiment.

Finally, it should be noted that for their boundary layer data analysis, George et al 1996 used a procedure which was the reverse of that used here. There a series of careful attempts was first made to obtain directly the variation of the parameters from the velocity profiles, then the friction law was inferred and shown to be in agreement with direct measurements. The fact that the procedure followed here has been equally successful lends credibility to both analyses, especially in view of the importance of the subtle difference in the friction law between the model proposed here and a simple log law with constant coefficients.

9 Acknowledgements

The authors are particularly grateful to Professor L. Smits and Dr. M. Zagarola for making their work available to us, and to M. Wosnik for helping to analyze the data.

References

[1] Barenblatt, G.J. (1978) *Similarity, Self-similarity, and Intermediate Asymptotics*, Plenum, NY.

[2] Barenblatt, G.J. (1993) Scaling laws for fully developed shear flow. Part 1, Basic hypotheses and analysis. *J. Fluid Mech.*, vol. 248, 513 –520.

[3] Barenblatt, G.J. and Prostokishnin, V.M. (1993) Scaling laws for fully developed shear flow. Part 2, Processing of Experimental Data. *J. Fluid Mech.*, vol. 248, 513 –520.

[4] Cole, J.D. and Kevorkian, J. (1981) *Perturbation Methods in Applied Mathematics*, Springer, NY.

[5] Gad-el-Hak, M. and Bandyopadhyay, P.R. (1994) Reynolds Number Effects in Wall-Bounded Flows, *Applied Mech. Rev., 47*, 307 –3365.

[6] George, W.K. (1995) Some New Ideas for Similarity of Turbulent Shear Flows, *Proc. of Lisbon Conf. on Turbulence and Turbulent Heat Transfer*, Hanjalic and Pereira, eds., Elsevier, Amsterdam.

[7] George, W.K. (1989) Self-Preservation of Turbulent Flows and Its Relation to Initial Conditions and Coherent Structures, in *Advances in Turbulence* (George and Arndt, eds.), 39 – 73, Hemisphere, NY.

[8] George, W.K. (1995) Some New Ideas for Similarity of Turbulent Shear Flows, *Proc. 1994 Conf. on Turbulence and Turbulent Heat Transfer*, Hanjalic and Peira, eds, Elsevier, Amsterdam.

[9] George, W.K. and Bower,D (1988) APS/DFD Meeting, Buffalo, NY.

[10] George, W.K. (1990) ASCE Mtg, San Diego.

[11] George, W.K., Knecht, P. and Castillo, L. (1992) The Zero-Pressure Gradient Boundary Layer Revisited, *13th Symposium on Turbulence* (Reed, X.B., ed.), Rolla, Mo.

[12] George, W.K., Castillo, L. and Knecht, P. (1992) The Zero-Pressure Gradient Boundary Layer Revisited, *13th Symposium on on Turbulence* (Reed, X.B., ed.), Rolla, Mo.

[13] George, W.K., Castillo, L. and Knecht, P. (1993, revised 1996) The Zero-Pressure Gradient Boundary Layer, *Reynolds Symposium on Turbulence*, Asilomar, CA, April.

[14] George, W.K. and Castillo, L. (1993) Boundary Layers with Pressure Gradient: Another Look at the Equilibrium Boundary Layer, *Near Wall Turbulent Flows*, (So, R.M.C. et al. editors), 901 – 910, Elsevier, NY.

[15] Hanjalic, K. and B.E. Launder (1974) Contribution towards a Reynolds stress closure for low-Reynolds number turbulence, Imp.Coll. Rept. HTS/74/24.

[16] Knecht, P. (1990) An Investigation of the Matched Layer in a Turbulent Boundary Layer with Zero Pressure Gradient, MS Thesis, Dept. Mech. & Aersp. Engr., SUNY/Buffalo, Buffalo, NY.

[17] Long, R.R. (1976) presentation at Naval Hydrodynamics Mtg., Wash., DC., June.

[18] Long, R.R. and Chen, T.-C. (1981) Experimental Evidence for the Existence of the 'Mesolayer' in Turbulent Systems, *J. Fluid Mech.*, 105, 19 – 59.

[19] Monin, A.S. and Yaglom, A.M. (1971) *Statistical Fluid Mechanics*, MIT Press, Cambridge, MA.

[20] Millikan, C.M. (1938) A critical discussion of turbulent flows in channels and circular tubes, *Proc. 5th Int. Congr. Appl. Mech.*, 386 – 392, Wiley, NY.

[21] Panton, R.(1990) Scaling Turbulent Wall Layers *J. Fluids Engr., 112*, 425 – 432.

[22] Prandtl, L. (1976) Zur Turbulenten Stroemung in Rohren und laengs Platten, *Ergeb. Aerod. Versuch Goettingen*, IV Lieferung, 18. (1932)

[23] Reynolds, W.C. (1976) Computation of Turbulent Flows, Ann. Rev. of Fluid Mech., 8, 183 –208.

[24] Stanton, T.E. and Pannell, J.R.(1914) Similarity of motion in relation to the surface friction of fluids, *Phil. Trans. Roy. Soc. A*, 214, p 199.

[25] Tennekes, H. and Lumley, J.L. (1972) *A First Course in Turbulence*, MIT, Cambridge.

[26] Tennekes, H. (1968) Outline of a Second-Order Theory of Turbulent Pipe Flow,*AIAA Jour.*, 6, 1735 – 1740.

[27] Zagorola, M.V. (1996) Ph.D Dissertation, Princeton U.

[28] Zagorola, M.V. and Smits, A.J. (1996) Scaling of the mean velocity profile for turbulent pipe flow. draft document.